First Measurement of Beta Decay Half-lives in Neutron-rich Tl and Bi Isotopes

Benzoni, G.; Morales, A. I.; Valiente-Dobon, J. J.; Gottardo, A.; Bracco, A.; Camera, F.; Crespi, F. C. L.; Corsi, A. M.; Leoni, S.; Million, B.; Nicolini, R.; Wieland, O.; Gadea, A.; Lunardi, S.; Boutachkov, P.; Bruce, A. M.; Gorska, M.; Grebosz, J.; Pietri, S.; Podolyak, Zs.; Pfuetzner, M.; Regan, P. H.; Weick, H.; Alcantara Nunez, J.; Algora, A.; Al-Dahan, N.; de Angelis, G.; Ayyad, Y.; Alkhomashi, N.; Allegro, P. R. P.; Bazzacco, D.; Benlliure, J.; Bowry, M.; Bunce, M.; Casarejos, E.; Cortes, M. L.; Bacelar, A. M. Denis; Deo, A. Y.; Domingo-Pardo, C.; Doncel, M.; Dombradi, Zs.; Engert, T.; Eppinger, K.; Farrelly, G. F.; Farinon, F.; Farnea, E.; Geissel, H.; Gerl, J.; Goel, N.; Gregor, E.

Published in:
Physics Letters. Section B: Nuclear, Elementary Particle and High-Energy Physics

DOI:
10.1016/j.physletb.2012.07.063

2012

First measurement of beta decay half-lives in neutron-rich Tl and Bi isotopes

G. Benzoni[a,*], A.I. Morales[a], J.J. Valiente-Dobón[b], A. Gottardo[b,c], A. Bracco[a,d], F. Camera[a,d], F.C.L. Crespi[a,d], A.M. Corsi[a,d,1], S. Leoni[a,d], B. Million[a], R. Nicolini[a,d], O. Wieland[a], A. Gadea[e], S. Lunardi[f,c], P. Boutachkov[g], A.M. Bruce[h], M. Górska[g], J. Grebosz[i], S. Pietri[g], Zs. Podolyak[j], M. Pfützner[k], P.H. Regan[j], H. Weick[g], J. Alcántara Núñez[l], A. Algora[e], N. Al-Dahan[j,2], G. de Angelis[b], Y. Ayyad[l], N. Alkhomashi[m], P.R.P. Allegro[n], D. Bazzacco[f], J. Benlliure[l], M. Bowry[j], M. Bunce[j], E. Casarejos[o], M.L. Cortes[g], A.M. Denis Bacelar[h], A.Y. Deo[j], C. Domingo-Pardo[g], M. Doncel[p], Zs. Dombradi[q], T. Engert[g], K. Eppinger[r], G.F. Farrelly[j], F. Farinon[g], E. Farnea[f], H. Geissel[g], J. Gerl[g], N. Goel[g], E. Gregor[g], T. Habermann[g], R. Hoischen[g,s], R. Janik[t], S. Klupp[r], I. Kojouharov[g], N. Kurz[g], S. Mandal[u], R. Menegazzo[f], D. Mengoni[f], D.R. Napoli[b], F. Naqvi[g,v], C. Nociforo[g], A. Prochazka[g], W. Prokopowicz[g], F. Recchia[f], R.V. Ribas[n], M.W. Reed[j], D. Rudolph[s], E. Sahin[b], H. Schaffner[g], A. Sharma[g], B. Sitar[t], D. Siwal[u], K. Steiger[r], P. Strmen[t], T.P.D. Swan[j], I. Szarka[t], C.A. Ur[f], P.M. Walker[j,3], H-J. Wollersheim[g]

[a] *Istituto Nazionale di Fisica Nucleare, Sezione di Milano, Milano, Italy*
[b] *Istituto Nazionale di Fisica Nucleare, Laboratori Nazionali di Legnaro, Legnaro, Italy*
[c] *Dipartimento di Fisica dell'Università degli Studi di Padova, Padova, Italy*
[d] *Dipartimento di Fisica dell'Università degli Studi di Milano, Milano, Italy*
[e] *Instituto de Física Corpuscular, CSIC-Universitat de València, València, Spain*
[f] *Istituto Nazionale di Fisica Nucleare, Sezione di Padova, Padova, Italy*
[g] *GSI Helmholtzzentrum für Schwerionenforschung, Darmstadt, Germany*
[h] *School of Computing, Engineering and Mathematics, University of Brighton, Brighton, United Kingdom*
[i] *Niewodniczanski Institute of Nuclear Physics, Polish Academy of Science, Krakow, Poland*
[j] *Department of Physics, University of Surrey, Guildford, United Kingdom*
[k] *Faculty of Physics, University of Warsaw, Warsaw, Poland*
[l] *Universidad de Santiago de Compostela, Santiago de Compostela, Spain*
[m] *KACST, Riyadh, Saudi Arabia*
[n] *Instituto de Fisica, Universidade de São Paulo, São Paulo, Brazil*
[o] *EEI, Universidade de Vigo, Vigo, Spain*
[p] *Grupo de Física Nuclear, Universidad de Salamanca, Salamanca, Spain*
[q] *Institute of Nuclear Research of the Hungarian Academy of Sciences, Debrecen, Hungary*
[r] *Physik Department, Technische Universität München, Garching, Germany*
[s] *Department of Physics, Lund University, Lund, Sweden*
[t] *Faculty of Mathematics and Physics, Comenius University, Bratislava, Slovakia*
[u] *Department of Physics and Astrophysics, University of Delhi, Delhi, India*
[v] *Institut für Kernphysik, Universität zu Köln, Köln, Germany*

Abstract

Neutron-rich isotopes around lead, beyond N=126, have been studied exploiting the fragmentation of an uranium primary beam at the FRS-RISING setup at GSI. For the first time β-decay half-lives of ^{219}Bi and ^{211,212,213}Tl isotopes have been derived. The half-lives have been extracted using a numerical simulation developed for experiments in high-background conditions. Comparison with state of the art models used in r-process calculations is given, showing a systematic underestimation of the experimental values, at variance from close-lying nuclei.

Keywords:
PACS: 23.40.-s, 26.30.Hj, 27.80.+w

The abundances of the natural elements observed in the Universe are fingerprints of the pathways and

*corresponding author
Email address: giovanna.benzoni@mi.infn.it (G. Benzoni)
[1] current address: CEA, Saclay, Fr.
[2] current address: Department of Physics, College of Science, University of Kerbala, Kerbala, Iraq
[3] current address: CERN, CH-1211 Geneva 23, Switzerland

timescales of the nucleosynthesis process. A reliable description of the underlying astrophysical scenarios depends crucially on the knowledge of nuclear properties in the relevant regions of the Segrè chart extending from nuclei close to stability, involved in the slow neutron capture process (s-process), up to nuclei far-off stability, approaching the neutron dripline in the case of the rapid neutron capture process (r-process) or the proton dripline in the case of the rapid proton capture process (rp-process) [1].

In this context, the half-lives of neutron-rich (n-rich) nuclei on the astrophysical r-process path are of primary importance for its full understanding [2]: they define how rapidly the heaviest nuclei are synthesized during the r-process, thus determining the strength of fission cycling [3, 4]. These half-lives define the matter-flow bottlenecks which largely influence the r-process abundance pattern. The r-process description is also affected by various inputs of nuclear properties such as masses, β-decay rates, (n,γ) and (γ,n) reaction cross sections, etc. Scarce experimental data on r-process nuclei [5, 6], contribute to the difficulties in understanding the astrophysical scenario.

Simulations of the r-process rely on theoretical models for the β-decay half-lives. These calculations have been done globally, i.e. for all r-process nuclei within the same framework, based on Quasi Particle Random-Phase Approximation (QRPA) on top of macroscopic-microscopic mass models like the Finite-Range Droplet Model (FRDM) [7], or on a self consistent microscopic approach as the one using the Fayans energy-density functional (DF3+cQRPA) [8]. The treatment of first forbidden (FF) transitions, found to be significant in particular for nuclei crossing the closed shells and having a neutron excess more than one major shell, is also different in both models. Whereas the FF strength is treated as a smooth background by the FRDM+QRPA [9], and thus included using the macroscopic phenomenological Gross Theory [10], the DF3+cQRPA treats FF decays microscopically, in terms of the reduced multipole operators depending on the space and spin variables [11].

Recent lifetime measurements on very n-rich nuclei nearby the $A \sim 130$ waiting-point [12] show an overestimation of a factor of two or more of the half-life calculations based on the FRDM+QRPA approach. Also the scarce data available approaching the $N = 126$ shell closure [13] indicate an overestimation of the lifetimes predicted by the same model, in this case of more than one order of magnitude. In contrast, the self-consistent description of the FF decays in the DF3+cQRPA framework predicts a stronger reduction of the half-lives, in better agreement with the experimental data.

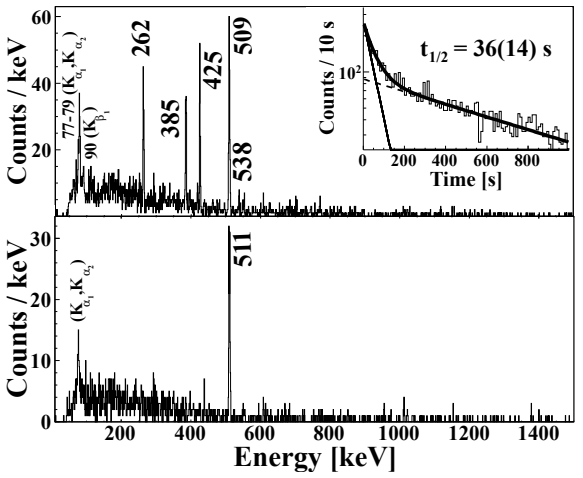

Figure 1: γ spectra correlated with the β decay of ^{218}Bi. In the top panel the correlations are performed in standard time sequence showing the expected γ-ray transitions from the known decay scheme [14] together with characteristic X rays. The bottom panel shows correlations performed in time reversal order to highlight random correlations. The inset in the panel shows the time distribution obtained in coincidence with the 262-, 385- and 425-keV transitions together with the analytical fit by a double component exponential-decay function, in order to account for the background.

The present letter reports on the first measurement of β-decay half-lives in ^{219}Bi and ^{211,212,213}Tl. The half-life of ^{218}Bi has been measured and compared to results obtained some years ago at CERN [14], and is therefore used as a test case for the analysis. Results in Tl (Z=81) and Bi (Z=83) isotopic chains are of particular importance since they lie at the two sides of the Z=82 proton shell closure. Even if not particularly n-rich, being just few neutrons away from the stability line, these are the most exotic nuclei so far accessible for spectroscopy studies. In this mass region predictions show a tendency to underestimate the measured values, at variance from the region below N=126, where the half-lives are overestimated.

The experimental data have been extracted using a numerical approach [15] which has been developed to study long-living nuclei, with half-lives of the order of tens of seconds. Issues related to the measurement of such long half-lives are strongly connected to a correct evaluation of the background, arising both from high implantation rates, giving rise to multiple, indistinguishable, implantations, and from activity build-up, owing to long correlation times.

The experiment has been performed exploiting a fragmentation reaction of a ^{238}U beam at 1 GeVA on a 2.5 g/cm^2 Be target. The ^{238}U beam was delivered by

Nucleus	Implanted ions	Implantation rate (s)	Efficiency $\epsilon_\beta * f$
^{219}Bi	2800	5.5×10^{-4}	0.20
^{218}Bi*	6678	0.013	0.44
^{213}Tl*	1526	1.9×10^{-4}	0.18
^{212}Tl	2768	4×10^{-4}	0.60
^{211}Tl	3503	4×10^{-4}	0.34

Table 1: Number of implanted ions (middle column) and corresponding implantation rates (right column) for the nuclei under analysis. Last column gives the product of the β-detection efficiency times the feeding of the states. See text for details. Half-lives of the nuclei marked with a star are already reported in literature [14, 16].

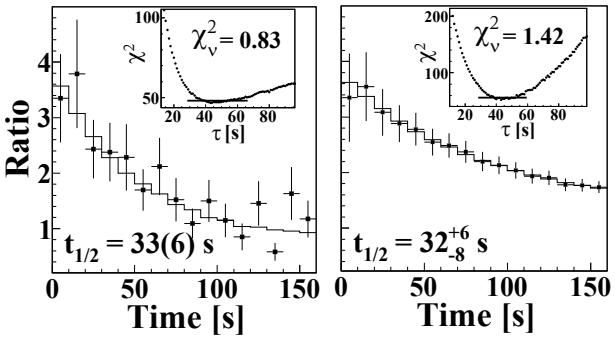

Figure 2: Experimentally (symbols) and numerically (solid lines) determined ratios between forward and backward time distributions for ^{218}Bi sorted in standard and accumulated format (left and right panel). In the insets the χ^2 minimization for the distributions are shown. (See text for details).

the UNILAC-SIS accelerator facilities at GSI at a stable intensity of 1.5×10^9 ions/spill, with a repetition cycle of 3 s and an extraction time of 1 s.

The nuclei of interest were separated and identified in the double-stage magnetic spectrometer FRagment Separator, FRS [17]. A 758 mg/cm^2 Al wedge-shaped degrader at the intermediate focal plane was set to produce a monochromatic beam, ensuring the implantation of the produced species in the active stopper located at the final focal plane of the FRS. Standard FRS equipment, comprising thin scintillator detectors in the intermediate and final focal plane for time of flight measurement, Time Projection Chambers for position determination and ionization chambers at the final focal plane for energy loss measurements, was employed. Two different FRS settings, centering on ^{215}Pb and ^{217}Pb, were measured, in order to populate the most exotic nuclei so far accessible in Pb, Tl and Bi isotopic chains. To reduce the count rate in the intermediate focal plane detectors, arising mainly from primary-beam charge states ($^{238}U^{91+}$ and $^{238}U^{90+}$), an additional homogeneous 2 g/cm^2 Al degrader was placed after the first dipole of the FRS. Further information on FRS settings for this experiment can be found in [18]. Details on the identification in mass over charge (A/q) and charge states discrimination are given in [19, 20].

At the final focal plane, the fragmentation residues were slowed down, in a variable-thickness Al degrader, to the energies required to implant the selected nuclei in the RISING active stopper, a composite DSSSD detector system comprising 3 layers, each with three DSSSD pads [21, 22]. Each DSSSD, 16 × 16 pixels, had dimensions 5 × 5 cm^2 and a thickness of 1 mm. The active stopper registered the position and time of an ion implantation and of the following β-decays. Two additional scintillator detectors were placed right in front and behind the silicon array to serve as software trigger and veto condition for an implantation event. The DSSSD detector system was surrounded by the RISING γ-ray spectrometer [23, 24], comprising 105 germanium crystals arranged in 15 clusters. The full-energy peak detection efficiency of the array was measured to be 15% at 662 keV [23]. This array enabled the measurement of γ-ray transitions in time coincidence with implantations and β-like particles, using a correlation time window of up to 100 μs.

A good implantation event was defined by a measured high energy signal in one pixel of the DSSSD pads. The particle-identification (Z,A), the pixel location and the implantation time, given by a timestamp module, were recorded. A matching β decay was defined as an event having an energy signal occurring in the pixel activated by the implantation, or in the neighboring cells, within a time-correlation window set according to the expected lifetime. An average of 60% matching β events happened in the 8 pixels adjacent to the one activated by the implantation, as expected by the range of electrons which is greater than the pixel size.

Due to the amount of δ-electrons produced during the stopping process of the residues in the Al degrader and in the Si detectors, only the β-like events recorded during the 2 s beam pause were considered, thus suppressing high-multiplicity "in-spill" correlations.

In order to reduce the background coming from the decay of the daughter nuclei and other nuclei implanted in the active stopper, the β-electrons were identified using the characteristic γ rays of the daughter nucleus, setting a time correlation window of 200 ns between β and γ decays. Owing to the uniqueness of the $\beta - \gamma$ correlations, this analysis does not need to include, in the

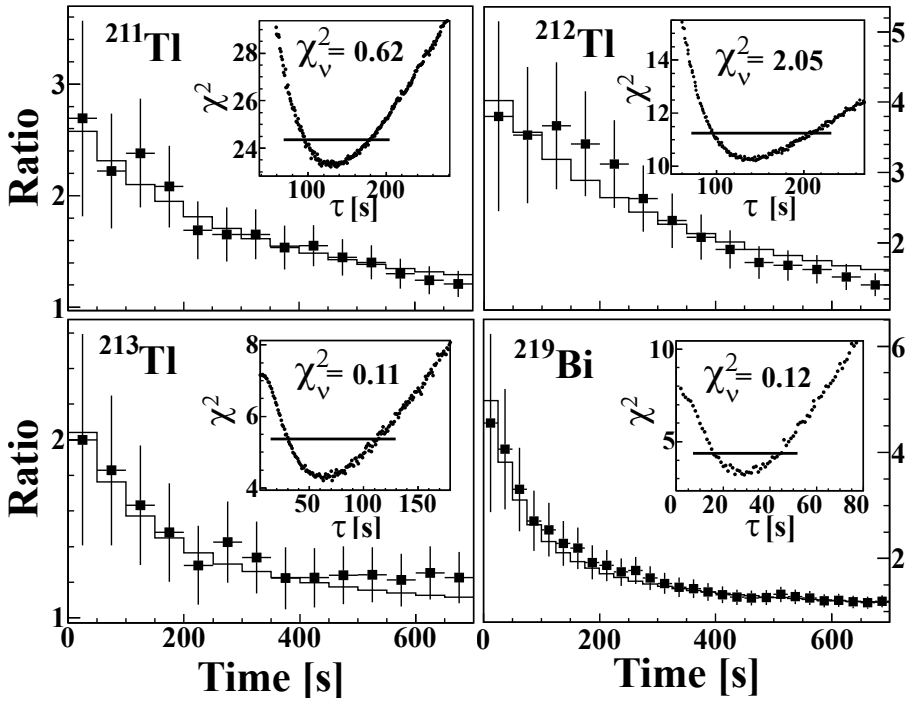

Figure 3: Experimentally (symbols) and numerically (solid lines) determined ratios between forward and backward distributions for ^{211,212,213}Tl and ^{219}Bi, together with the χ^2 minimization in the insets. Resulting half-lives are given in the text.

evaluation of the half-life, the decay of daughter and grand-daughter nuclei, which would have comparably long lifetimes. Following this procedure, the first accepted β-like event occurred after the ion implantation corresponds to the real decay with the maximum probability.

Table 1 reports the number of implanted ions for each of the isotopes under analysis, together with the typical implantation rate.

Figure 1 shows β-delayed γ spectra referring to the decay ^{218}Bi $\rightarrow^{218}$Po. In order to evaluate the background contributions, the ion-β correlations were sorted both in the correct time sequence (the "forward" spectrum in the top panel) and in time-reverse mode (the "backward" spectrum in the bottom panel). The "forward" spectrum shows transitions that have been attributed to the decay of ^{218}Bi in Ref. [14], together with characteristic X rays, while the "backward" spectrum shows predominantly contributions from the X-rays and the annihilation peak at 511 keV. The inset shows the experimental decay curve obtained for the 262-, 385-, and 425-keV lines. The analytical fit to exponential functions, also displayed in the figure with the solid line, returns a half-life of 36(14) s for this decay, well in agreement with the previously reported value of 33(1) s. The uncertainty of the present measurement embodies both the error of the analytical fit and the systematic errors related to the bin size of the experimental time distribution and the suppression of "in-spill" correlations.

The suppresion of such "in-spill" correlations in the experimental time distributions has been investigated using the new numerical approach described in [15]. This method has been developed to study long-time ion-β correlations in high-background experiments. The complex spill structure of the experiment is a critical issue considering that the half-lives under study span more than one beam repetition cycle. In contrast to the analytical fit, this procedure considers all the possible background sources by simulating the experimental sequences of implantations and decays. The numerical approach consists in performing a χ^2 fit between the experimental data and a series of numerical functions, obtained from Monte Carlo simulations of the ion-β-γ time correlations, for which the decay lifetime τ is the only free parameter. As the number of γ rays (N_γ) and implantations (N_I) were extracted from the recorded data, the total detection efficiency of γ-labelled electrons could be easily determined for each nuclear species according to $N_\gamma = \epsilon_\gamma * \epsilon_\beta * f * N_I$, where ϵ_γ and ϵ_β are the γ- and β-detection efficiencies, while f accounts

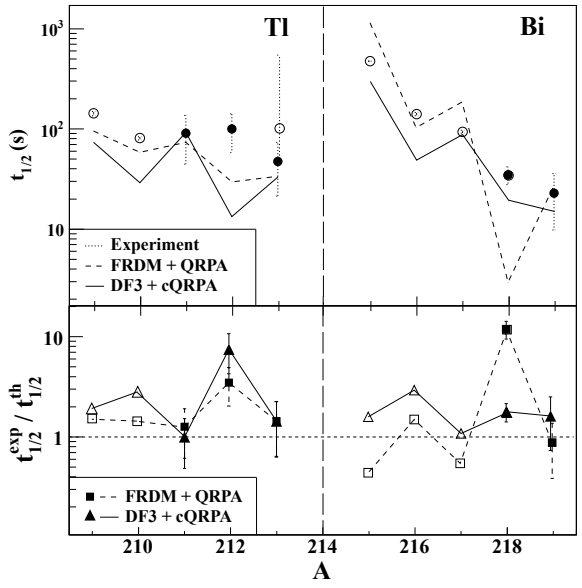

Figure 4: Comparison with theoretical predictions. In the upper row the half-lives are given as function of mass number A for Tl (left) and Bi (right) isotopes. Open circles refer to previously known data while filled ones to the current analysis. The lower panels show the comparison in terms of ratio between experimental and theoretical values. The predictions shown by squares are obtained using the FRDM+QRPA approach while the ones shown with triangles by the DF3+cQRPA one. (See text for discussion).

for the feeding of the states populated in the daughter nucleus. Typical values for the γ-detection efficiencies ranged between 15% to 20%, according to γ-ray energies. In table 1 we quote the product of $\epsilon_\beta * f$ used for the nuclei under analysis.

The uncorrelated contributions are evaluated by sorting the experimental (and simulated) data with a time-reversed sequence of ion-β-γ correlations, and are considered in the χ^2 test by using, as fitting function, the ratio between "forward" and "backward" time correlations.

The forward to backward ratios of the time distributions of ^{218}Bi are shown in Fig. 2. Experimental values are reported by symbols while the simulated ones, corresponding to the lifetime τ that minimizes the χ^2 test, by full lines. In order to increase the statistics of long-time correlations the data have been sorted also in the so-called "accumulated" format, adding the statistics of previous bins. In the insets of Fig. 2 the χ^2 minimization and the half-life extracted from the procedure in the two cases are shown. The horizontal lines account for statistical error corresponding to a variation of 1 unit in the χ^2 minimization.

Results from the numerical approach are in good agreement both with the analytical value extracted from the data and the previously published result [14].

Once verified the reliability of the analysis technique, the half-lives of other nuclear species, for which specific coincident γ transitions were observed, have been obtained. The resulting half-lives are: 22^{+7}_{-7} s for ^{219}Bi, 88^{+46}_{-29} s for ^{211}Tl, 96^{+42}_{-38} s for ^{212}Tl, 46^{+55}_{-26} s for ^{213}Tl. In the case of ^{213}Tl we significantly improve the precision on this measurement compared to the previously reported value, 101^{+484}_{-46}s, extracted during a mass measurement using time-resolved Schottky spectrometry [16].

Figure 3 shows the results of the numerical fit for the above mentioned nuclei. Again in this figure symbols represent the measured forward-backward ratios, while the full lines the best-fitting simulated ratios. The χ^2 minimizations are shown in the insets. The measurement of these half-lives is of great importance being these nuclei the most exotic so far accessible in this mass region. Details on $\beta - \gamma$ correlations for these nuclei will be given in a forthcoming publication.

Figure 4 shows the comparison of the experimental data with the theoretical approaches described in the introduction [9, 11]. Both models underestimate the half-lives by factors ranging from 1.5 to 10, except for the odd-mass Bi isotopes for which the FRDM+QRPA predicts higher values. In this case, the agreement with the experimental data improves for the most neutron-rich nuclei.

First-forbidden transitions play a crucial role in the description of the decay of neutron-rich nuclei in this mass region and predictions come very close to the experimental values. The need of the inclusion of first forbidden transitions can be understood also considering the involved orbitals. The major FF contribution is related to the $(\nu 1i_{11/2}\pi 1h_{9/2})$, $(\nu 3d_{5/2}\pi 2f_{7/2})$ and the slightly hindered $(\nu 2g_{9/2}\pi 1h_{9/2})$, $(\nu 2g_{9/2}\pi 2f_{7/2})$ configurations, thus predicting a strong competition between high transition energy GT and FF decays. In the case of the Tl isotopes, the $3s_{1/2}$, $2d_{3/2}$ orbitals in the proton valence space are partially opened, favouring highly energetic Gamow-Teller (GT) transitions from the partially occupied $4s_{1/2}$, $3d_{5/2}$ neutron shells. Also the expected relatively high Q_β values (3.5-6.0 MeV) open the stretched $(\nu 1i_{11/2}\pi 1i_{13/2})$ quasiparticle configuration, giving rise to a non-negligible GT strength [11, 25].

The modelization is, however, not perfect, since the models show, for instance, a staggering between odd and even nuclei that is not as strong in the experimental data. Moreover predictions deviate when passing through the N=126 shell closure: experimental data are

on average overestimated in case of N<126 [13], while they are underestimated in nuclei with neutron number N>126. For some specific nuclei the predictions seem to fail drammatically: an example is ^{218}Bi, whose half-life, confirmed in the present analysis, is not reproduced in the FRDM+QRPA treatment even with the inclusion of FF transitions, or the case of ^{212}Tl which is heavily underestimated by both approaches.

Given the presented discrepancies, further β-decay studies at both sides of the N=126 shell closure are highly demanded.

The results presented in this letter on the measurement of half-lives in ^{219}Bi and ^{211,212,213}Tl are important to extrapolate the behavior of nuclei in the proximity of the r-process path. Theoretical calculations are here shown to generally underestimate the half-lives for these heavy n-rich nuclei. If this situation persists for even more exotic systems, this will have implications on the r-process timescale and abundances, which, in turn, affect the amount of U and Th produced, as well as the amount and timescale of the reprocessing through fission.

The excellent work of GSI accelerator staff is acknowledged. The authors acknowledge the support of INFN, Italy and MICINN, Spain, through the AIC10-D-000568 bilateral action. A.G. and A.A. activity has been partially supported by MICINN, Spain and the Generalitat Valenciana, Spain, under grants FPA2008-06419-C02-01 and PROMETEO/2010/101. The support of the UK STFC and AWE plc, and of the DFG(EXC 153) is also acknowledged.

References

[1] K.Langanke, F.-K.Thielemann, M.Wiescher, The Euroschool Lectures on Physics with Exotic Beams vol.1 (Lecture Notes in Physics vol 651), Springer, 2004.
[2] J. J. Cowan, et al., Phys. Rep. 208 (1991) 267.
[3] I. V. Panov, et al., Nucl.Phys. A747 (2005) 633.
[4] F. K. Thielemann, Z. Phys. A309 (1983) 301.
[5] R. L. Gill, et al., Phys. Rev. Lett. 56 (1986) 1874.
[6] A. Jungclaus, et al., Phys. Rev. Lett. 99 (2007) 132501.
[7] P. Möller, J. R. Nix, K.-L. Kratz, Atomic Data and Nuclear Data Tables 66 (1997) 131.
[8] I. N. Borzov, et al., Z. Phys. A 355 (1996) 117.
[9] P. Möller, B.Pfeifer, K.-L. Kratz, Phys. Rev.C 67 (2003) 055802.
[10] K. Takahashi, M. Yamakada, Prog. Theo. Phys. 41 (1969) 1470.
[11] I. N. Borzov, Phys. Rev. C67 (2003) 025802.
[12] S. Nishimura, et al., Phys. Rev. Lett. 106 (2011) 052502.
[13] T. Kurtukian-Nieto, et al., Nucl. Phys. A827 (2009) 587c.
[14] H. De Witte, et al., Phys. Rev. C69 (2004) 044305.
[15] T. Kurtukian-Nieto, et al., Nucl. Instr. Meth. A589 (2008) 472.
[16] L. Chen, et al., PLB 691 (2010) 234.
[17] H. Geissel, et al., Nucl. Instr. Meth. B70 (1992) 286.
[18] A. Gottardo, et al., 2012. Submitted to PRL.
[19] A. I. Morales, et al., Phys. Rev. C84 (2011) 011601.
[20] N. Alkhomashi, et al., Phys. Rev. C80 (2009) 064308.
[21] R. Kumar, et al., Nucl. Instr. Meth. A598 (2009) 754.
[22] P. H. Regan, et al., Int. J. Mod. Phys. E 17 (2008) 8.
[23] S. Pietri, et al., Nucl. Instr. Meth. B261 (2007) 1079.
[24] P. H. Regan, et al., Nucl. Phys. A787 (2007) 491c.
[25] I. N. Borzov, Nucl.Phys. A645 (2006) 777.